



## Study of Photocatalytic Degradation of Methylene Blue Dye with green Synthesized Maghemite Nanoparticles Using Aqueous Extract of Brassica Tournfortii Leaves

Wedad Mohammed Barag<sup>1\*</sup>, Fatma Ali Shtewi<sup>2</sup>, Wedad Melad Al-Adiwish<sup>3</sup>, Awatif AbdUlsalam Tarroush<sup>4</sup>

<sup>1,2,3,4</sup> Chemistry Department, Faculty of Science, University of zawia, Libya

دراسة التحفيز الضوئي لتحلل صبغة أزرق الميثيلين باستخدام جسيمات الماغيميت النانوية المُصنَّعة بواسطة المستخلص المائي لأوراق نبات العسلوز

وداد محمد برق<sup>1\*</sup>، فاطمة علي الشتيوي<sup>2</sup>، وداد ميلاد الاديوش<sup>3</sup>، عواطف عبد السلام طروش<sup>4</sup>  
<sup>1,2,3,4</sup> قسم الكيمياء، كلية العلوم، جامعة الزاوية، ليبيا

\*Corresponding author: [w.barag@zu.edu.ly](mailto:w.barag@zu.edu.ly)

Received: March 31, 2026

Accepted: May 14, 2026

Published: June 11, 2026

### Abstract:

Water pollution has been a major concern for environmentalists worldwide, especially pollution by organic dyes, because dyes are harmful to the environment and ultimately human health. In present study, the Brassica tournfortii was first carried out as the reducing and stabilizing agents via a green approach for the synthesis of maghemite nanoparticles ( $\gamma$ -Fe<sub>2</sub>O<sub>3</sub>NPs) and evaluated their significant methylene blue dye photocatalytic degradation. The  $\gamma$ -Fe<sub>2</sub>O<sub>3</sub>NPs were characterized using UV-Vis, FT-IR, XRD and SEM techniques. According to UV-Vis spectra, SPR band at 442 nm with band gap energy about 2.65 eV, as well as the surface functional groups of biomolecules identified by FT-IR. The XRD confirmed the cubic crystalline structure of  $\gamma$ -Fe<sub>2</sub>O<sub>3</sub>NPs with a crystallite size of 13.85 nm. While SEM revealed spherical and uniform morphology. The  $\gamma$ -Fe<sub>2</sub>O<sub>3</sub>NPs exhibited potential photocatalytic efficiency by degrading 80.12 % of a 10 ppm Methylene blue (MB) dye solution within 90 min under sunlight irradiation, following pseudo second-order kinetic. The presented results revealed that the  $\gamma$ -Fe<sub>2</sub>O<sub>3</sub>NPs are attractive photocatalyst for developing effective water purification for organic dyes.

**Keywords:** Brassica Tournfortii leaves extract,  $\gamma$ -Fe<sub>2</sub>O<sub>3</sub>NPs, Photocatalytic Degradation, Methylene Blue dye, Sunlight Irradiation.

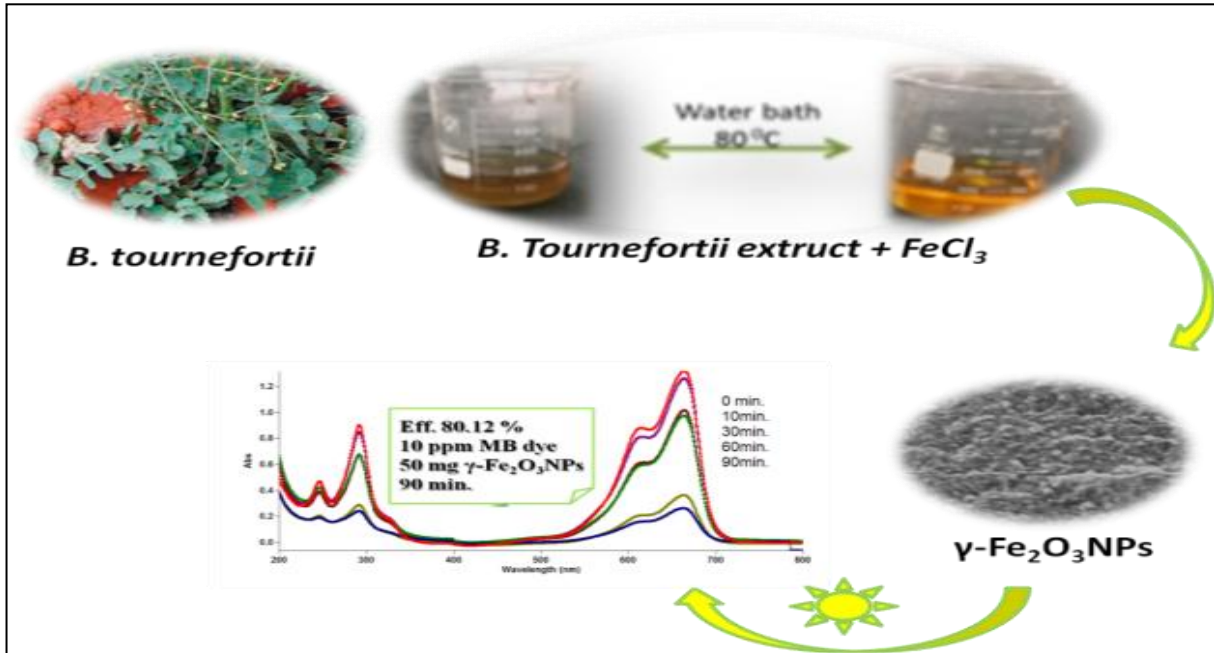
### المخلص

يُعدّ تلوث المياه مصدر قلق بالغ للمهتمين بالبيئة في جميع أنحاء العالم، ولا سيما التلوث بالأصبغ العضوية، نظرًا لضرر هذه الأصبغ بالبيئة وصحة الإنسان. في هذه الدراسة، تم لأول مرة استخدام مستخلص أوراق نبات العسلوز كعوامل مختزلة ومثبتة لاصطناع جسيمات الماغيميت النانوية ( $\gamma$ -Fe<sub>2</sub>O<sub>3</sub>NPs) باستخدام الاصطناع الأخضر، وتقدير فعاليتها في التحفيز الضوئي لتحلل لصبغة الميثيلين الأزرق. تم توصيف  $\gamma$ -

$\text{Fe}_2\text{O}_3\text{NPs}$  باستخدام تقنيات الأشعة فوق البنفسجية المرئية، والأشعة تحت الحمراء، وحيود الأشعة السينية، والمجهر الإلكتروني الماسح. أظهرت أطياف الأشعة فوق البنفسجية المرئية وجود حزمة رنين بلازمون سطحي عند 442 نانومتر، مع طاقة فجوة نطاق تبلغ حوالي 2.65 إلكترون فولت، بالإضافة إلى المجموعات الوظيفية السطحية للجزيئات الحيوية التي تم تحديدها بواسطة الأشعة تحت الحمراء. أكد حيود الأشعة السينية أن بنية  $\gamma\text{-Fe}_2\text{O}_3\text{NPs}$  البلورية مكعبة وبحجم بلوري يبلغ 13.85 نانومتر. بينما كشف المجهر الإلكتروني الماسح عن شكل كروي منتظم. أظهرت  $\gamma\text{-Fe}_2\text{O}_3\text{NPs}$  كفاءة تحفيز ضوئي عالية، حيث تحلل 80.12% من محلول صبغة أزرق الميثيلين (MB) بتركيز 10 جزء في المليون خلال 90 دقيقة تحت أشعة الشمس، وفقاً لحركية تفاعل من الرتبة الثانية الوهمية. كما أظهرت النتائج المعروضة أن جسيمات  $\gamma\text{-Fe}_2\text{O}_3\text{NPs}$  هي محفز ضوئي جذاب لتطوير تنقية المياه الفعالة للأصبغ العضوية.

**الكلمات المفتاحية:** مستخلص أوراق نبات *Brassica Tournefortii*، جسيمات نانوية من  $\gamma\text{-Fe}_2\text{O}_3$ ، التحلل الضوئي التحفيزي، صبغة أزرق الميثيلين، الإشعاع الشمسي.

### Graphical Abstract



### 1. INTRODUCTION

Iron oxide nanoparticles (IONPs) have attracted much concern owing to their unique properties, such as superparamagnetism, surface-to-volume ratio, greater surface area, a propensity to agglomerate and easy separation methodology [1]. Iron oxides exist in nature in many forms, which are hematite ( $\alpha\text{-Fe}_2\text{O}_3$ ), maghemite ( $\gamma\text{-Fe}_2\text{O}_3$ ) wustite (FeO) and magnetite ( $\text{Fe}_3\text{O}_4$ ), being most probably common and important technologically [2]. Among them, maghemite nanoparticles ( $\gamma\text{-Fe}_2\text{O}_3\text{NPs}$ ) have attracted particular interest for biomedical applications such as therapeutic and diagnostic applications [2, 3]. Furthermore, maghemite nanoparticles ( $\gamma\text{-Fe}_2\text{O}_3\text{NPs}$ ) are an attractive n-type semiconductor with band gap of 2.0 eV and a spinel structure [4]. Accordingly, it had significant environmental applications such as the removal of heavy metals and photocatalytic degradation of industrial dyes from wastewater [5-7]. To synthesis of  $\gamma\text{-Fe}_2\text{O}_3\text{NPs}$ , many methods can be considered, including sonication-calcination method [8], co-precipitation [9], hydrothermal synthesis [10], thermal

decomposition [11], and sol–gel method [12]. However, these methods are usually expensive and labor-intensive and are potentially hazardous to the environment and living organisms. Therefore, using the phytochemicals present in plants as bio-reductants is attaining a greater impetus. Various plants have been studied for the green synthesis of  $\gamma$ -Fe<sub>2</sub>O<sub>3</sub>NPs such as *Ziziphus jujuba* [7], *Prosopis farcta* [13], *taranjabin* [14], *E. platyloba* [15] and *pheonix dactylifera* [16]. However, there are no reports on the formation of iron oxide nanoparticles using *Brassica tournefortii* plant. *Brassica tournefortii* (*B. tournefortii*) is a locally known as African mustard or Sahara mustard, belongs to the family Brassicaceae. *Brassica tournefortii* is an annual herbaceous plant, native to the North Africa and Middle East [17]. It contains a huge spectrum of various secondary metabolites (glucosinolates, carotenoids, isothiocyanates and polyphenols compounds) and is rich of vitamins and minerals [18].

Recently, successful green synthesis of silver and copper oxide nanomaterials using *Brassica tournefortii* leaves has been reported. Our research group has synthesized silver nanowires (AgNWs) using an aqueous extract of *Brassica tournefortii* leaves and evaluated their antibacterial and antioxidant activities [19]. Similarly, the green synthesis and antibacterial activity of copper oxide nanoparticles (CuONPs) using an aqueous extract of *Brassica tournefortii* leaves also has been reported [20].

Methylene blue (MB) dye is a cationic organic chloride salt with the cation 3,7 bis(dimethylamino) phenothiazin-5-ium. Methylene blue dye is recognized as a popular cationic dye utilized in a variety of sectors, including the pharmaceutical, food processing, paint, medicine and textile industry [5]. Methylene blue dye is harmful to the environment due to its poisonous and carcinogenic. The threshold value for methylene blue in the water is about 5–10 mg/L [21], thus requiring the development of an efficient method to reduce organic dyes, include adsorption, chemical precipitation, filtration, ion-exchange, coagulation/flocculation, reverse osmosis, and electrodialysis; unfortunately, these methods have high operating costs and are ineffective in accomplishing the total elimination of organic dyes from wastewater [22]. Photocatalysis is more advantageous than other methods since it remains the most economical, reduces pollution, no secondary pollution occurs [7], eco-friendly and widely uses.

In this study, we successfully synthesized  $\gamma$ -Fe<sub>2</sub>O<sub>3</sub> nanoparticles through a rapid, simple, and eco-friendly method, without any hazardous chemicals as reducing or stabilizing agents. The goal of this study has been to synthesize maghemite nanoparticles ( $\gamma$ -Fe<sub>2</sub>O<sub>3</sub>NPs) using an aqueous extract of *Brassica tournefortii* leaves, and this synthesized  $\gamma$ -Fe<sub>2</sub>O<sub>3</sub>NPs employed for the photocatalytic degradation of methylene blue dye under sunlight Irradiation.

## 2. EXPERIMENTAL PART

### 2.1 materials

Fresh leaves of *Brassica tournefortii* plant were collected from Az-Zāwiyah, Libya. Ferric chloride hexahydrate (FeCl<sub>3</sub>.6H<sub>2</sub>O), Sodium hydroxide (NaOH) and methylene blue dye were purchased from sigma Aldrich.

## 2.2 Preparation of *Brassica tournefortii* leaves extract

The fresh *Brassica tournefortii* leaves were collected from Zawiya city, north Libya (March 2025). The leaves were thoroughly washed several times using normal water and then followed by distilled water to remove impurities. The (10 g) of leaves were cut into fine pieces and boiled with 100 ml of distilled water for 15 minutes. Then, the extract was filtered through Whatmann paper (size No.1). Finally, the aqueous extract was stored at 4°C for future work [19].

## 2.3 Green synthesis of maghemite nanoparticles

For the green synthesis of  $\gamma$ -Fe<sub>2</sub>O<sub>3</sub>NPs, aqueous extract of *Brassica tournefortii* leaves was added to 0.01M of FeCl<sub>3</sub>.6H<sub>2</sub>O solution in a 1:1 (v/v) ratio followed by pH adjustment to 9 by 0.1 M sodium hydroxide solution, and the mixture was stirred for 1 hour at 80°C. The formation of brown colloidal solution is indicating the formation of  $\gamma$ -Fe<sub>2</sub>O<sub>3</sub>NPs. The colloidal solution was centrifuged at 3000 r/m for 15 minutes to get the powdered nanoparticles, which washed thoroughly with distilled water and ethanol to remove the unwanted organic matter and air-dried at room temperature for 48 hours. Finally, the  $\gamma$ -Fe<sub>2</sub>O<sub>3</sub>NPs was calcinated in electronic oven at 400 °C for 2 hours. The Schematic diagram of the green synthesis of  $\gamma$ -Fe<sub>2</sub>O<sub>3</sub>NPs is shown in Figure 1.

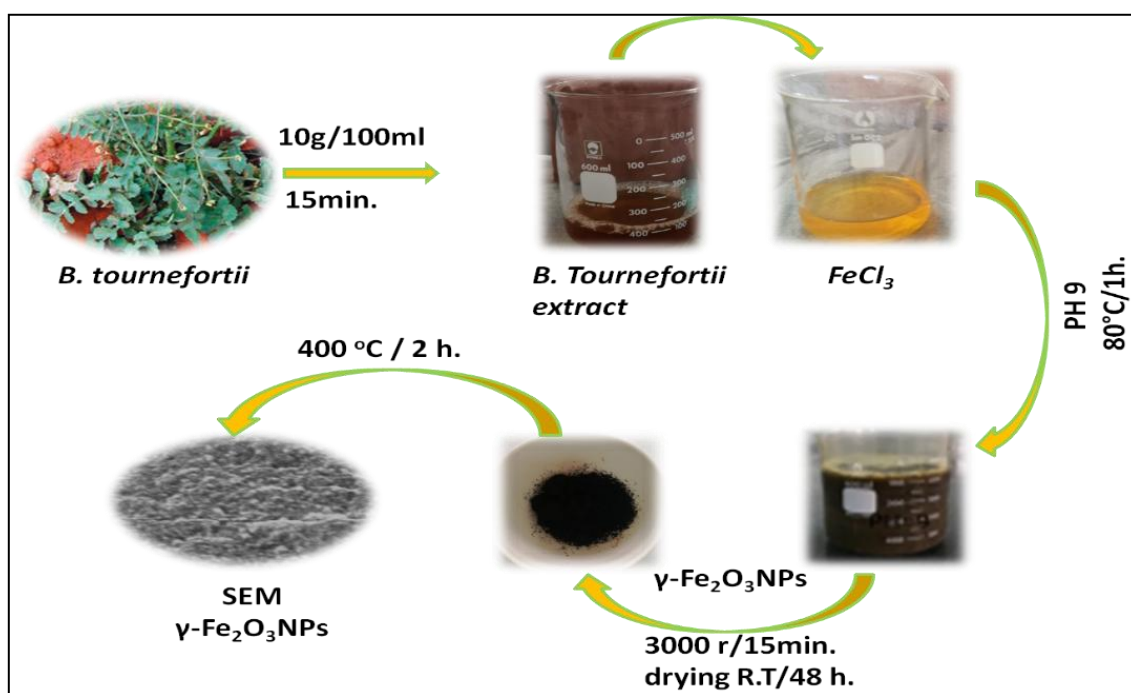


**Figure 1.** Schematic diagram of green synthesized  $\gamma$ -Fe<sub>2</sub>O<sub>3</sub>NPs

## 2.4 Chemical characterizations

UV–vis spectrophotometer (JASCO V 670) was used to monitor the green synthesis of  $\gamma$ -Fe<sub>2</sub>O<sub>3</sub>NPs. The respective SPR peaks were recorded between 200 and 800 nm. The obtained powdered  $\gamma$ -Fe<sub>2</sub>O<sub>3</sub>NPs were analyzed by FT-IR (IR Affinity-1s (Shimadzu) spectrometer), recorded in the wavenumber range of 500–4,000 cm<sup>-1</sup> to find the functional groups present around the synthesized  $\gamma$ -Fe<sub>2</sub>O<sub>3</sub>NPs. The crystal structure of the sample was analyzed by using XRD (Shimadzu XRD-6100 diffractometer) with a Cu K $\alpha$  radiation monochromatic filter in

the range 35–80°. Then, the size of  $\gamma$ -Fe<sub>2</sub>O<sub>3</sub>NPs was calculated using Scherer equation. The morphology of the synthesized  $\gamma$ -Fe<sub>2</sub>O<sub>3</sub> NPs were observed by scanning electron microscopy (SEM, LEO 1430VP).

### 2.5 Photocatalytic degradation study

In photocatalytic degradation study of  $\gamma$ -Fe<sub>2</sub>O<sub>3</sub>NPs, the methylene blue dye (MB) removal was performed using a 10 ppm methylene blue solution (100 mL) and 50 mg of  $\gamma$ -Fe<sub>2</sub>O<sub>3</sub>NPs catalyst. The mixtures were kept in the dark condition under stirring and followed with photocatalytic irradiation sunlight to measure the extent of the dye's adsorption onto the catalyst's surface. The solution was taken every 30 min intervals, and the absorbance of each methylene blue solution was measured using a UV-Vis spectrophotometer [22]. Similar steps were repeated for all samples. The percent degradation of MB was calculated using the Equation (1).

$$\% \text{ Deg.} = [(C_0 - C_t)/C_0] * 100 \quad (1)$$

where % Deg. is the degradation efficiency, C<sub>0</sub> and C<sub>t</sub> are defined as the concentration (mg/L) of MB solution before and after sunlight irradiation, respectively. The  $\lambda_{\text{max}}$  of the MB solution was recorded to be 664 nm.

## 3. RESULTS AND DISCUSSION

### 3.1 UV-Vis Spectroscopy analysis

The color change is the preliminary conformation study for the formation of  $\gamma$ -Fe<sub>2</sub>O<sub>3</sub>NPs. During the reaction, when an aqueous extract of *Brassica tournefortii* leaves was added to iron chloride solution (FeCl<sub>3</sub>.6H<sub>2</sub>O), and pH is adjusted to 9, the color of FeCl<sub>3</sub>.6H<sub>2</sub>O solution changes from pale yellow to brown and then to brown black, as shown in Figure 1. The phytoconstituents of *Brassica tournefortii* leaves extract is sufficient to reduce Fe<sup>3+</sup> ions to  $\gamma$ -Fe<sub>2</sub>O<sub>3</sub>NPs which acts as a reducing and stabilizing agent. The formation and reduction process was monitored by UV-Vis spectrometry. The synthesized  $\gamma$ -Fe<sub>2</sub>O<sub>3</sub>NPs have significant absorption bands between 200 and 800 nm. Figure 2 UV-Vis spectra showed a broad single absorbance band at 442 nm corresponded to the characteristic surface plasmon resonance (SPR) of  $\gamma$ -Fe<sub>2</sub>O<sub>3</sub>NPs, which is similar to the previous literatures [15,16].

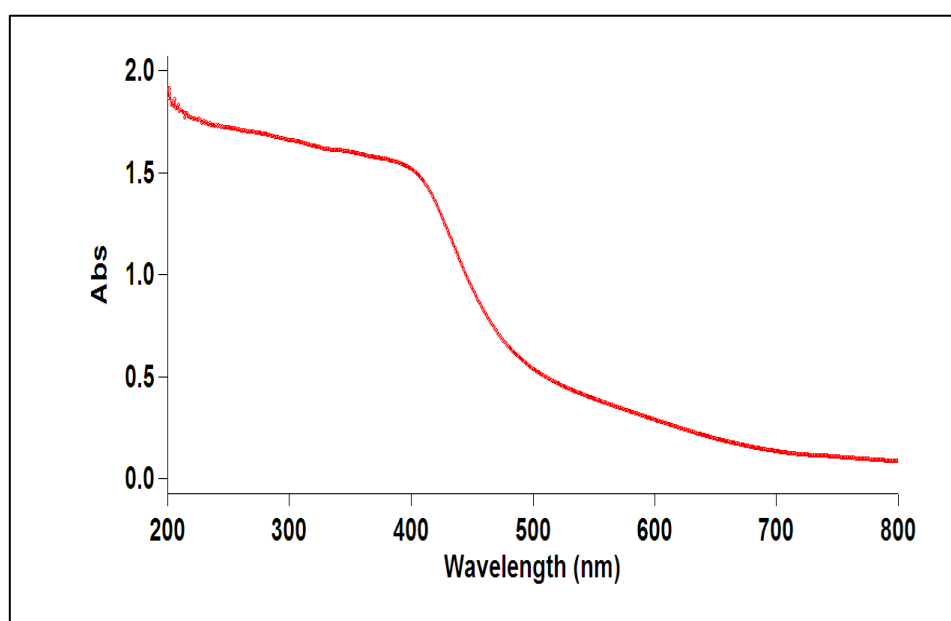


**Figure 2.** UV-Vis spectra of  $\gamma$ -Fe<sub>2</sub>O<sub>3</sub>NP

The optical band energy of nano-catalyst is an important factor for photo-catalytic activity. The energy of incident light is provided by a nano-catalyst with band gap energy equal to or greater than that of photocatalyst. When enough electrons are stimulated from the valence band (VB) to the conduction band (CB), the photocatalytic behavior of the catalyst will be productive. The band gap ( $E_g$ ) value of the  $\gamma$ - $Fe_2O_3$ NPs has been studied and calculated according to Tauc equation [23].

$$\alpha hv = A(hv - E_g)^{0.5} \quad (2)$$

where  $\alpha$  is the absorption coefficient,  $E_g$  is band gap energy,  $A$  is constant and  $hv$  is the photon energy. Plotting  $(\alpha hv)^2$  versus  $(hv)$  plot and linearly regressing the linear portion of the  $(\alpha hv)^2$  to zero. The optical band gap of  $\gamma$ - $Fe_2O_3$ NPs are shown in Figure 3. The plots of  $(\alpha hv)^2$  versus  $(hv)$  for  $\gamma$ - $Fe_2O_3$ NPs. The band gap energy of the  $\gamma$ - $Fe_2O_3$ NPs was measured by extrapolating the linear portion of the plot to the energy axis and is found to be of the order of 2.65 eV. The direct optical band gap of  $\gamma$ - $Fe_2O_3$ NPs has been calculated as 2.65 eV, which can be lower than to priyadarshi et al. [24] where the maghemite nanoparticles band gap was found 3.9 eV. The slight difference in the calculated value may be attributed to the size of the nanoparticles due to the quantum confinement effect.

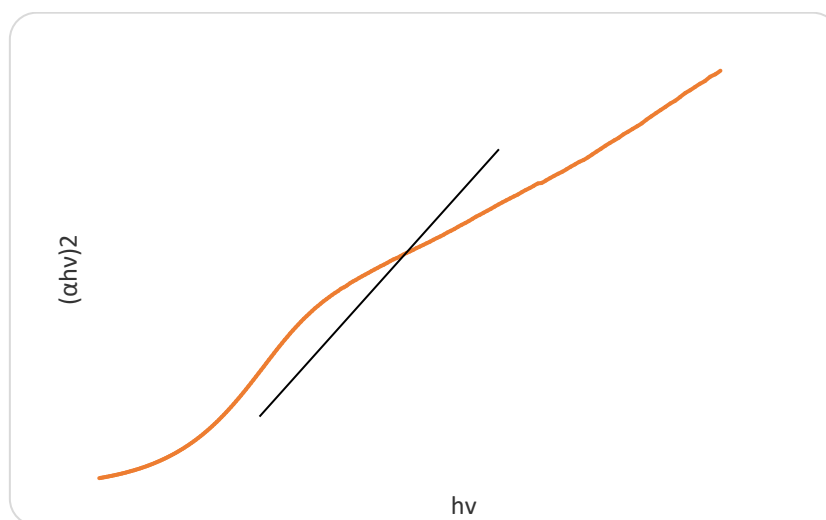


**Figure 3.** optical band gap energy of  $\gamma$ - $Fe_2O_3$ NP

### 3.2 FT-IR Analysis and Probable Mechanism of $\gamma$ - $Fe_2O_3$ NP

The FT-IR spectra of *Brassica tournefortii* and  $\gamma$ - $Fe_2O_3$ NPs were investigated in range 500–4000, as shown in Figure 4. Characterizing the surface functional groups of  $\gamma$ - $Fe_2O_3$ NPs by FT-IR spectroscopy explains the association of phytochemical components of *Brassica tournefortii* with the  $\gamma$ - $Fe_2O_3$ NPs. As shown in Figure 4A, a broad absorption band at region 3100-3300  $cm^{-1}$  indicated to (–OH) stretching vibration of polyphenols and amide (–NH) stretching of the protein component. The peaks at 3027, 2919, and 2850  $cm^{-1}$  attributed to the (C–H) stretching of the aromatic ring, asymmetric, and symmetric stretching of aliphatic hydrocarbon, respectively. Moreover, the peak in the range 1736 and 1595  $cm^{-1}$  shows the presence of (C=O) stretching vibrations and (–C=C–) in the aromatic ring. The peaks at 1428 and 1245  $cm^{-1}$  correspond to the (C–N) and (O–H) stretching vibrations of polyphenol. The intense peaks at 1143 and 1065  $cm^{-1}$  depict (C–O) stretching of phenolic compounds. A band at 838  $cm^{-1}$  related to aromatic ring vibration.

The successful capping of the *Brassica tournefortii* onto the surface of  $\gamma$ -Fe<sub>2</sub>O<sub>3</sub>NPs can be confirmed by FT-IR spectra of  $\gamma$ -Fe<sub>2</sub>O<sub>3</sub>NPs, presented in Figure 3B, reveals the presence of surface O-H groups as indicated by a peak at 3189 cm<sup>-1</sup>. However, these bands demonstrated shifts and broadening due to overlapping with the O-H stretching band present on the surface of  $\gamma$ -Fe<sub>2</sub>O<sub>3</sub>NPs. Additionally, the 1557cm<sup>-1</sup> and 1386 cm<sup>-1</sup> peaks correspond to C=O and C-O stretching vibrations, respectively, indicating the presence of biomolecules acting as capping agents to stabilize the  $\gamma$ -Fe<sub>2</sub>O<sub>3</sub>NPs. Maghemite band is observed between 600 and 635 cm<sup>-1</sup>. Therefore, Fe-O stretches at the 635 cm<sup>-1</sup> belongs to the maghemite nanoparticles [5,7, 15]. The results of the present study indicated the successful synthesis of  $\gamma$ -Fe<sub>2</sub>O<sub>3</sub>NPs from *Brassica tournefortii* leaves extract.

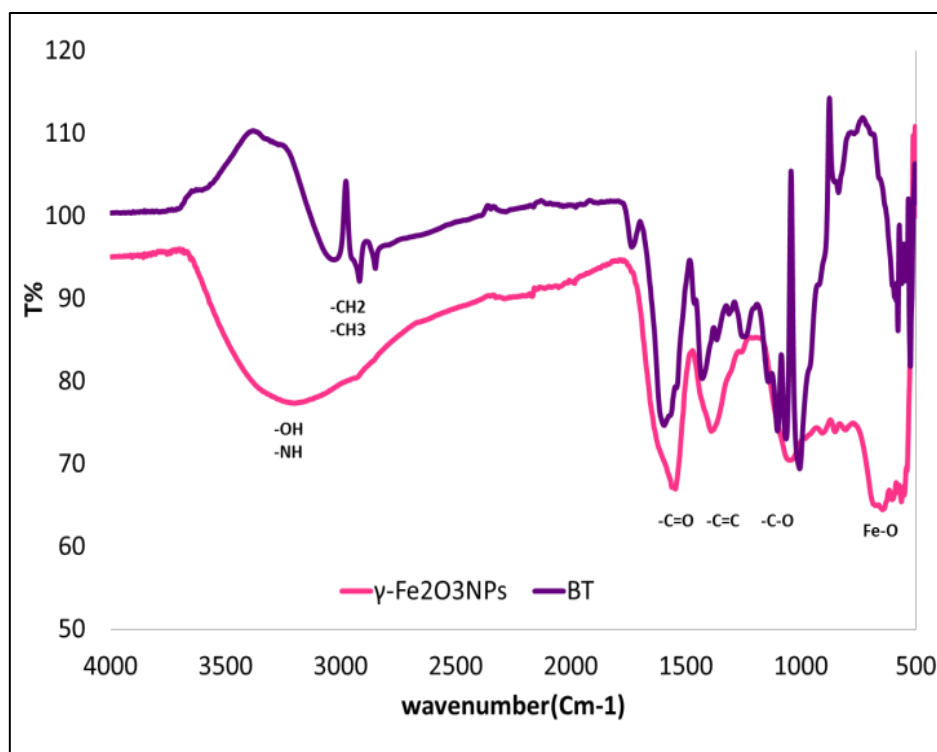
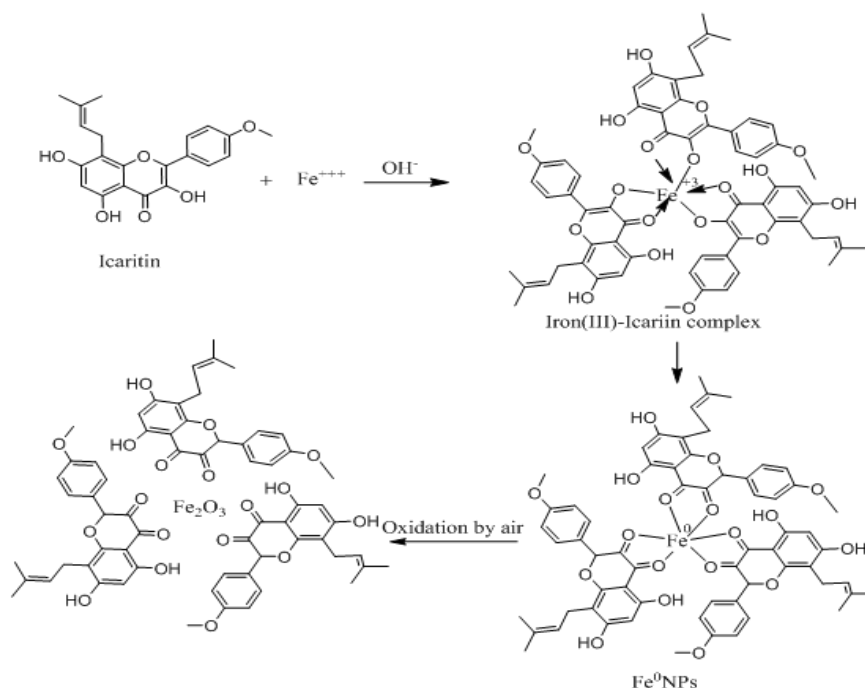


**Figure 4.** FT-IR spectra of (a) *Brassica tournefortii* leaves and (b)  $\gamma$ -Fe<sub>2</sub>O<sub>3</sub>NPs

#### Probable Mechanism of green synthesized $\gamma$ -Fe<sub>2</sub>O<sub>3</sub> NPs

The exact mechanism of green synthesized  $\gamma$ -Fe<sub>2</sub>O<sub>3</sub>NPs remains challenges. The plausible mechanism of  $\gamma$ -Fe<sub>2</sub>O<sub>3</sub>NPs is schematically presented in Scheme 1. Rahmani et al. [18] reported that the leaves of *Brassica tournefortii* richness by several isothiocyanates and polyphenols include icariin, L-tyrosine 7-amido-4-methylcoumarin, Polydatin, 3',5'-dihydroxyflavone, Phenoxodiol. Among these phytoconstituents, icariin reached as the highest concentration with 2.3 mg/g of in the leaves of *Brassica tournefortii*. The phytoconstituents could act as reducing and stabilizing agent for the synthesis of nanoparticles [19]. Accordingly, icariin is possible that plays the main role in the formation of  $\gamma$ -Fe<sub>2</sub>O<sub>3</sub>NPs. The icariin will be hydrolysis to icaritin. Then, the hydroxyl groups of icaritin contained in the extract are deprotonated and are made stronger as a complexing and reducing agent for the iron ions. Subsequently, the Fe<sup>3+</sup> ions oxidized the hydroxyl groups into carbonyl groups in the reduction reaction as the iron ions were reduced to the zero-valent iron nanoparticles that are oxidized due to the exposure to air resulting in  $\gamma$ -Fe<sub>2</sub>O<sub>3</sub>NPs. A similar mechanism was previously reported by our research group for synthesized AgNWs using *Brassica tournefortii* extract [19].



**Scheme 1.** Plausible mechanism of green synthesized  $\gamma$ - $\text{Fe}_2\text{O}_3$  NPs.

### 3.3 XRD analysis

Figure 5 shows the X-ray diffraction pattern of the green synthesized  $\gamma$ - $\text{Fe}_2\text{O}_3$  NPs calcinated at 400 °C for 2 hours. The  $\gamma$ - $\text{Fe}_2\text{O}_3$  NPs exhibited the diffraction peaks at 30.08°, 36.18°, 43.85°, 45.45°, 47.97° and 63.45°, correspond to the (220), (311), (400), (422), (511) and (440) for cubic spinel  $\gamma$ - $\text{Fe}_2\text{O}_3$  NPs powder phase. The resulted peaks and their corresponding Bragg's reflections are strongly agreed with the (JCPDS, file no. 00-039-1346) [25]. From the XRD pattern, it can be observed that some extra diffraction peaks corresponding to  $\alpha$ - $\text{Fe}_2\text{O}_3$ , as reported in previous studies [15, 26]. The high peak intensity of (311) at  $2\theta=36,18^\circ$  with narrow full width at half maximum (FWHM) illustrates the good crystalline nature of synthesized the maghemite. The crystallite size of 13.85 nm was estimated by using the Debye-Scherrer equation.

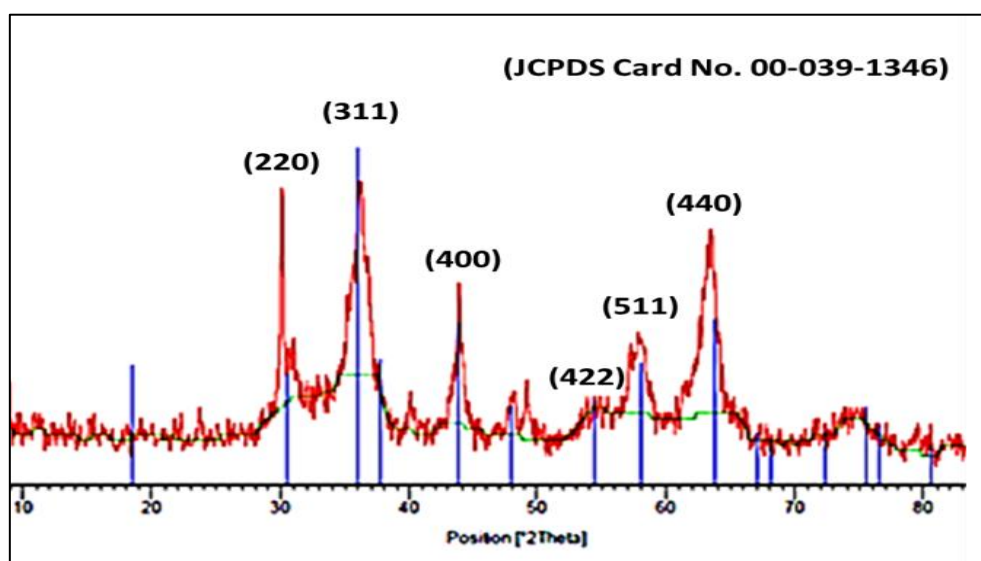


**Figure 5.** XRD pattern of the green synthesized  $\gamma$ - $\text{Fe}_2\text{O}_3$  NPs

### 3.4 SEM analysis

Scanning electron microscopy (SEM) played a key role to explore the size and morphology of the nanomaterials because their catalytic and biological behavior strongly depends on size and shape. Figure 6 shows SEM images of the green synthesized  $\gamma$ -Fe<sub>2</sub>O<sub>3</sub>NPs. Figure 6(a) shows the SEM image regarding  $\gamma$ -Fe<sub>2</sub>O<sub>3</sub>NPs, which were air-dried at room temperature for 48 hours and then calcinated in the electronic oven at 400 °C for 2 hours. The SEM image of  $\gamma$ -Fe<sub>2</sub>O<sub>3</sub>NPs showed that majority of the nanoparticles was in spherical shape and uniform in size. The image revealed that the particles were agglomerated, which might be due to the magnetic interactions between the nanoparticles. Similar results have also been reported by Cao et al. [26]. In contrast, Figure 6 (b) illustrates the SEM micrograph of the  $\gamma$ -Fe<sub>2</sub>O<sub>3</sub>NPs, which was prepared without an air-dried at room temperature and then calcinated in the electronic oven at 400 °C for 2 hours. It revealed that the particle size becomes non uniform, nearly spherical in shape with agglomeration due to reduce surface free energy.

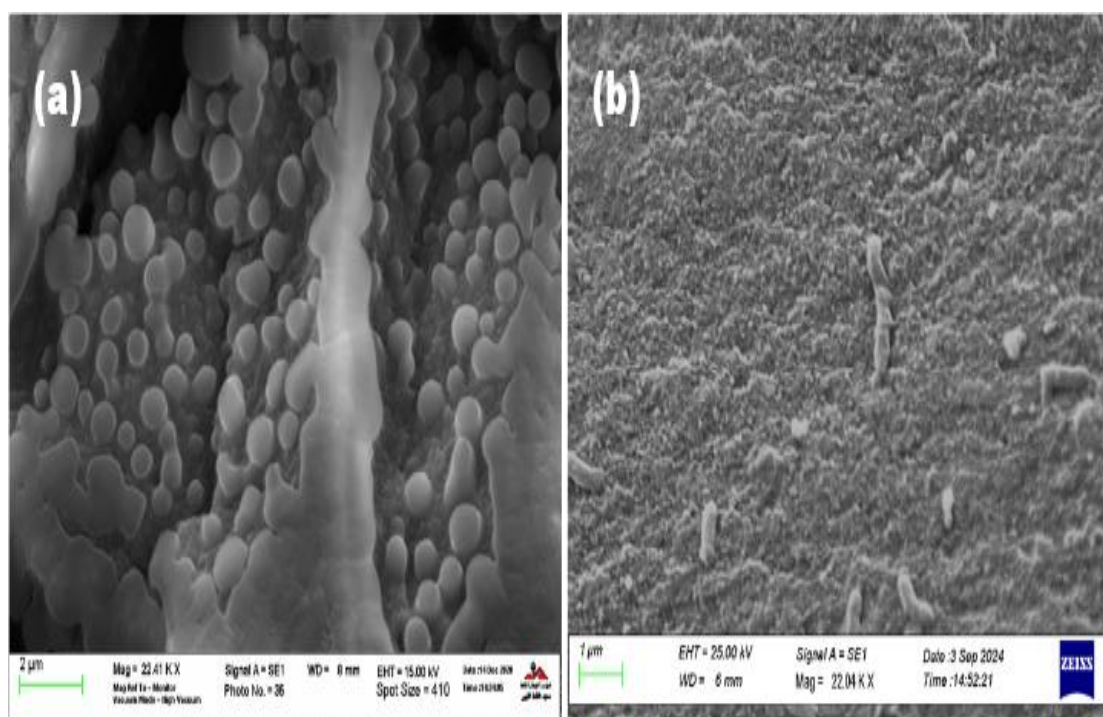


**Figure 6.** The SEM images of green synthesized of  $\gamma$ -Fe<sub>2</sub>O<sub>3</sub>NPs (a) with air-dried at r.t (b) without air-dried at r.t.

### 3.5 Photocatalytic Degradation study

The photocatalytic degradation of MB dye using green synthesized  $\gamma$ -Fe<sub>2</sub>O<sub>3</sub>NPs as efficient photocatalyst is shown in Figure 7. In order to investigate the photocatalytic activity of  $\gamma$ -Fe<sub>2</sub>O<sub>3</sub>NPs, the applied test condition included pH = 8, 50 mg of  $\gamma$ -Fe<sub>2</sub>O<sub>3</sub>NPs and 10 ppm of MB dye concentration. MB is a synthetic basic dye with sensitive oxidation/reduction properties [5]. The common ionic form is monomeric (MB<sup>+</sup>) in water, which can create dimers and trimers. The observed two absorbance peaks 664nm and 292 nm, respectively. The absorbance peak at 664 nm, corresponds to (n -  $\pi^*$ ) transitions (monomeric (MB<sup>+</sup>) form), which is reduced to dark blue colour to colourless due to electron transfer. Furthermore, the absorbance peak at 290 nm confirmed the ( $\pi$  -  $\pi^*$ ) transitions [27].

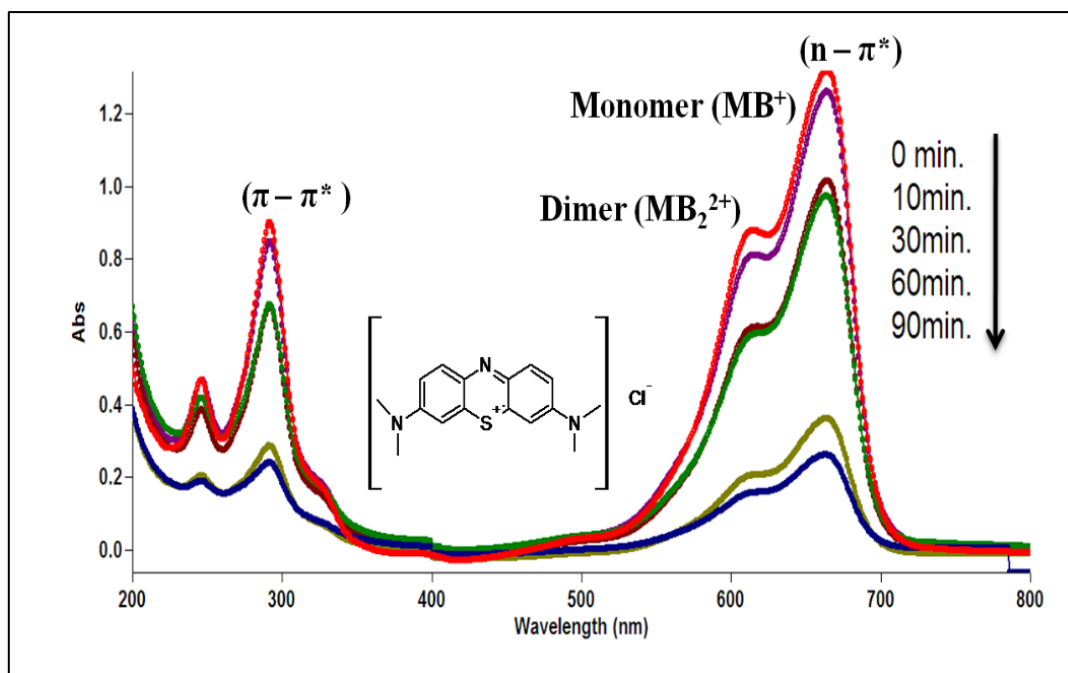


**Figure 7** photocatalytic degradation of MB dye using green synthesized  $\gamma\text{-Fe}_2\text{O}_3$ NPs

**Figure 8** displays the percentage of degradation of MB dye at different time interval of the  $\gamma\text{-Fe}_2\text{O}_3$ NPs. Under dark adsorption, the  $\gamma\text{-Fe}_2\text{O}_3$ NPs showed removal efficiency at 4.4% within 30 min (before sunlight irradiation). The removal efficiency was further enhanced to reach 80.12 % within 90 min under sunlight irradiation. Miri et al., [7] observed that the synthesized  $\gamma\text{-Fe}_2\text{O}_3$ NPs NPs using aqueous extract of *Ziziphus jujube* degraded about 92.8% of methylene blue dye during 160 minutes under sunlight irradiation.

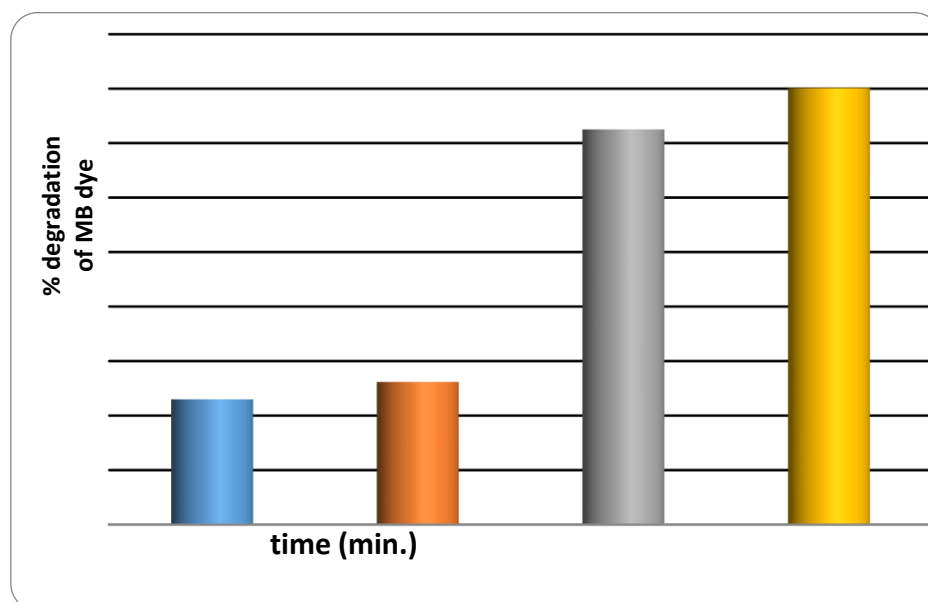


**Figure 8** The percentage of degradation of MB dye at different time interval of green synthesized  $\gamma\text{-Fe}_2\text{O}_3$ NPs.

The kinetic experiment for MB dye degradation was carried out under optimized conditions using the absorbance of dye solution measured at 0, 10, 30, 60 and 90 min. The kinetic of methylene blue adsorption on  $\gamma\text{-Fe}_2\text{O}_3$ NPs was evaluated using the pseudo-first-order Equation (3) and the pseudo-second-order Equation (4).

$$\ln(q_e - q_t) = \ln q_e - k_1 t \quad (3)$$

$$t/q_t = \frac{1}{k_2(q_e)^2} + \frac{t}{q_e} \quad (4)$$

where  $k_1$  ( $\text{min}^{-1}$ ) and  $k_2$  are the rates of sorption ( $\text{g} \cdot \text{mg}^{-1} \cdot \text{min}^{-1}$ ),  $q_e$  is the amount of methylene blue removed at equilibrium ( $\text{mg} \cdot \text{g}^{-1}$ ), and  $q_t$  is the amount of methylene blue removed at  $t$  time ( $\text{mg} \cdot \text{g}^{-1}$ ). Figure 9 and Table 1 showed that green synthesized  $\gamma\text{-Fe}_2\text{O}_3\text{NPs}$  followed the pseudo-second model rather than the pseudo-first-order model.

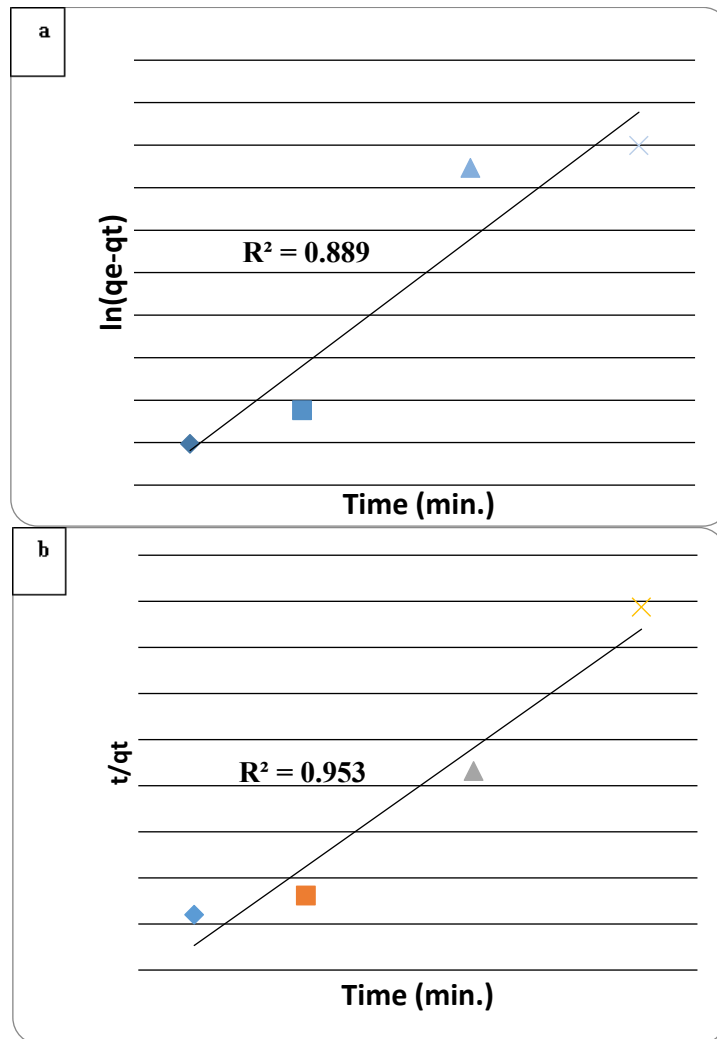


**Figure 9** a) Pseudo first-order kinetic b) Pseudo second-order kinetic for photocatalytic degradation of MB dye using green synthesized  $\gamma\text{-Fe}_2\text{O}_3\text{NPs}$

**Table 1.** Data of kinetics model of Pseudo first order and second order for green synthesized  $\gamma\text{-Fe}_2\text{O}_3\text{NPs}$

|                      | <b>pseudo-first order</b> | <b>pseudo-second order</b> |
|----------------------|---------------------------|----------------------------|
| <b>K</b>             | <b>0.019</b>              | <b>4.289</b>               |
| <b>R<sup>2</sup></b> | <b>0.889</b>              | <b>0.953</b>               |

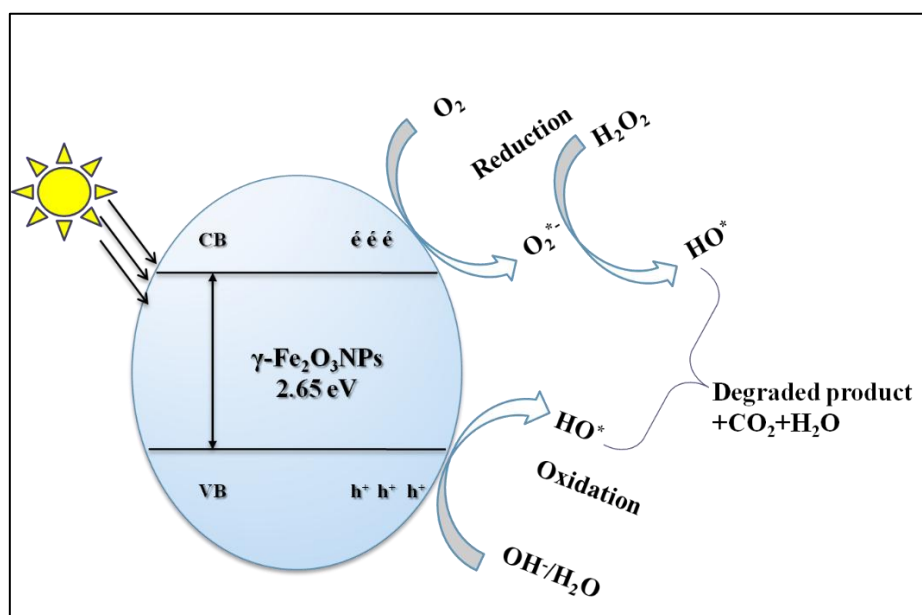
### 3.5.1 Proposed mechanism of MB dye photocatalytic degradation

Figure 10 shows proposed mechanism of MB dye photocatalytic degradation using green synthesized  $\gamma\text{-Fe}_2\text{O}_3\text{NPs}$ . During degradation, when excited by sunlight generates electron-hole pairs on the surface of the  $\gamma\text{-Fe}_2\text{O}_3\text{NPs}$  at band gap equals to 2.65 eV, both hydroxyl radicals ( $\text{HO}^\bullet$ ) and superoxide anion radicals ( $\text{O}_2^{\bullet-}$ ) are formed by the reaction of charge carriers ( $e^-/h^+$  pairs) with  $\text{H}_2\text{O}$  and  $\text{O}_2$ . The hydroxyl radicals play an important role in the degradation of methylene blue dye [28]. These free radicals of high reactivity and high oxidation potential may react with methylene blue dye, converting it into nontoxic products such as degraded compounds, carbon dioxide and water [29], as shown in a series of following reactions:

- $\gamma\text{-Fe}_2\text{O}_3\text{ NPs} + h\nu \rightarrow \gamma\text{-Fe}_2\text{O}_3\text{ NPs} (e^- + h^+)$
- $\text{H}_2\text{O}/\text{OH}^- + \gamma\text{-Fe}_2\text{O}_3\text{ NPs} (h^+) \rightarrow \text{OH}^\bullet + \text{H}^+ + \gamma\text{-Fe}_2\text{O}_3\text{ NPs}$
- $\gamma\text{-Fe}_2\text{O}_3\text{NPs} (e^-) + \text{O}_2 \rightarrow \text{O}_2^{\bullet-} + \text{H}^+$
- $\text{O}_2^{\bullet-} + \text{H}^+ \rightarrow \text{HO}_2^\bullet$
- $2 \text{HO}_2^\bullet \rightarrow \text{H}_2\text{O}_2 + \text{O}_2$
- $\text{H}_2\text{O}_2 \rightarrow \text{OH}^- + \text{OH}^\bullet$
- $\text{H}_2\text{O}_2 + \gamma\text{-Fe}_2\text{O}_3\text{ NPs} (e^-) \rightarrow \text{OH}^\bullet + \text{OH}^- + \gamma\text{-Fe}_2\text{O}_3\text{ NPs}$

The MB dye molecules absorb energy and are excited by transferring electrons by produce  $\text{Fe}^{2+}$ , as shown in the following reaction [28,30]:

- $\text{MB Dye} + h\nu \rightarrow \text{MB}^\bullet\text{Dye}$
- $\text{MB}^\bullet\text{Dye} + \gamma\text{-Fe}_2\text{O}_3\text{ NPs} \rightarrow \gamma\text{-Fe}_2\text{O}_3\text{ NPs} + \text{MB Dye}^{\bullet+}$
- $\text{OH}^\bullet + \text{MB}^\bullet\text{Dye}^{\bullet+} \rightarrow \text{Degradation product} + \text{CO}_2 + \text{H}_2\text{O}$
- 



**Figure 10** Proposed mechanism for photodegradation of MB using green synthesized  $\gamma\text{-Fe}_2\text{O}_3\text{ NPs}$

#### 4. CONCLUSION

From the results it can be concluded that an eco-friendly, efficient, and nontoxic method was used to synthesize maghemite nanoparticles using aqueous ferric chloride solution as precursor and the aqueous extract of *Brassica tournefortii* leaves as a reducing and stabilizing agents. The green synthesized  $\gamma$ -Fe<sub>2</sub>O<sub>3</sub>NPs optical, structural and morphological characteristics were investigated using UV-Vis, FTIR, XRD, and SEM techniques. The green synthesized  $\gamma$ -Fe<sub>2</sub>O<sub>3</sub>NPs exhibited potential photocatalytic activity towards the degradation of methylene blue dye on exposing to sunlight irradiation. The degradation effectiveness against methylene blue dye was found to be 80.12% within 90 min. Based on the findings of this study; the green synthesized  $\gamma$ -Fe<sub>2</sub>O<sub>3</sub>NPs can be used as efficient photocatalyst for water treatment technology.

#### ABBREVIATIONS

$\gamma$ -Fe<sub>2</sub>O<sub>3</sub>NPs: maghemite nanoparticles  
SPR: Surface plasmon resonance  
FT-IR: Fourier transform infrared spectroscopy  
UV-Vis: Ultraviolet–visible spectroscopy  
XRD: X-ray diffraction analysis  
SEM: Scanning electron microscopy  
MB dye: Methylene blue dye

#### AUTHOR INFORMATION

Wedad Mohamed Barag: <https://orcid.org/0000-0002-8134-6999>

Fatma Ali Shtewi: <https://orcid.org/0009-0007-8113-8536>

Awatif Abd Tarroush: <https://orcid.org/0009-0004-4563-7248>

Wedad M. Al-Adiwish: <https://orcid.org/0000-0002-1442-1477>

#### AUTHOR CONTRIBUTIONS

All authors contributed to the study conception and design. Material preparation, data collection and analysis were performed by Barag W.M., Shtewi F. A., Tarroush A.A.U., Al-Adiwish W.M. The first draft of the manuscript was written by Barag W.M. and Shtewi F. A. All authors have read and agreed to the published version of the manuscript.

#### CONFLICT OF INTERESTS

The authors declare that they have no conflict of interest.

#### ACKNOWLEDGMENTS

The authors are grateful to the Department of Chemistry at Zawia University and Libyan Medical Research Center in Zawia for providing lab facilities and equipment to perform this study. Petroleum Training & Qualifying Institute in Tripoli for providing the XRD &SEM, and Polymer Research Center in Tripoli for providing FT-IR.

---

#### *Disclosure of conflict of interest*

The authors declare that they have no conflict of interest.

---

#### References

- [1] N. Ajinkya, X. Yu, P. Kaithal, H. Luo, P. Somani and S. Ramakrishna, “Magnetic Iron Oxide Nanoparticle (IONP) Synthesis to Applications: Present and Future”, *Materials*, vol. 13, pp. 4644. 2020 doi: [10.3390/ma13204644](https://doi.org/10.3390/ma13204644).
- [2] K. N. Shoudho, S. Uddin, M.M. H.Rumon, M.S. Shakil, “Influence of Physicochemical Properties of Iron Oxide Nanoparticles on Their Antibacterial Activity”, *ACS Omega*, vol. 9, pp.33303–33334, 2024 doi: [10.1021/acsomega.4c02822](https://doi.org/10.1021/acsomega.4c02822)

- [3] Zúñiga-Miranda, J.; Guerra, J.; Mueller, A.; Mayorga-Ramos, A.; Carrera-Pacheco, S.E.; Barba-Ostria, C.; Heredia-Moya, J.; Guamán, L.P. “Iron Oxide Nanoparticles: Green Synthesis and Their Antimicrobial Activity”, *Nanomaterials*, vol, 13, pp. 2919, 2023. [doi: 10.3390/nano13222919](https://doi.org/10.3390/nano13222919)
- [4] N.A. Yousif, S. M. H. Al-Jawad, A.A. Taha, H. Stamatis, “A Review of Structure, Properties, and Chemical Synthesis of Magnetite Nanoparticles”, *Journal of Applied Sciences and Nanotechnology*, vol. 3, pp. 18-31, 2023 [doi: 10.53293/jasn.2022.5179.1178](https://doi.org/10.53293/jasn.2022.5179.1178)
- [5] R. Thakur, N. Kaur, M. Kaur, P.K. Bhowmik, H. Han, K. Singh, F.M. Husain, H.S. Sohal, “Green Synthesis of Magnetic Fe<sub>2</sub>O<sub>3</sub> Nanoparticle with *Chenopodium glaucum* L. as Recyclable Heterogeneous Catalyst for One-Pot Reactions and Heavy Metal Adsorption”. *Molecules* vol.29, pp.4583, 2024 [doi: 10.3390/molecules29194583](https://doi.org/10.3390/molecules29194583)
- [6] L. Doan, “Modifying Superparamagnetic Iron Oxide Nanoparticles as Methylene Blue Adsorbents: A Review”. *Chem. Engineering* vol.7, pp.77, 2023 . [doi: 10.3390/chemengineering7050077](https://doi.org/10.3390/chemengineering7050077)
- [7] A. Miri, A.S. Sedighi, A. Najafidoust, M. Khatami, M. sarani, “Study of photodegradation performance and ability of lead removal of green synthesized maghemite nanoparticles Using *Ziziphus Jujuba* Extract”. *Int J Environ Anal Chem.* Vol.103, pp. 8369–8383, 2023. [doi: 10.21203/rs.3.rs-545585/v1](https://doi.org/10.21203/rs.3.rs-545585/v1)
- [8] L. M. Khoiroh, F. Khidin, R. Ningsih, “Synthesis of Maghemite ( $\gamma$ -Fe<sub>2</sub>O<sub>3</sub>) nanoparticles pigment from lathe waste by sonication – calcination method”. *IOP Conf. Ser.: Earth Environ. Sci.*, vol. pp.012005, 2020 [doi:10.1088/1755-1315/456/1/012005](https://doi.org/10.1088/1755-1315/456/1/012005)
- [9] N. Tabassum, V. Singh, V.K. Chaturvedi, E. Vamanu, M.P. Singh, A “Facile Synthesis of Flower-like Iron Oxide Nanoparticles and Its Efficacy Measurements for Antibacterial, Cytotoxicity and Antioxidant Activity”. *Pharmaceutics*, vol.15, pp. 1726, 2023. [doi: 10.3390/pharmaceutics15061726](https://doi.org/10.3390/pharmaceutics15061726)
- [10] V. Sreeja, P. A. Joy, “Microwave-hydrothermal synthesis of  $\gamma$ -Fe<sub>2</sub>O<sub>3</sub> nanoparticles and their magnetic properties”, *Materials Research Bulletin*, vol. 42, pp. 1570–1576, 2007 [doi: 10.1016/j.materresbull.2006.11.004](https://doi.org/10.1016/j.materresbull.2006.11.004).
- [11] W. Zhou, K. Tang, S. Zeng, Y. Qi, “Room temperature synthesis of rod-like FeC<sub>2</sub>O<sub>4</sub>·2H<sub>2</sub>O and its transition to maghemite, magnetite and hematite nanorods through controlled thermal decomposition”, *Nanotechnology*, vol.19, pp.065602, 2008 [doi: 10.1088/0957-4484/19/6/065602](https://doi.org/10.1088/0957-4484/19/6/065602).
- [12] J. Parhizkar, M. H. Habibi, “Synthesis, characterization and photocatalytic properties of Iron oxide nanoparticles synthesized by sol-gel autocombustion with ultrasonic irradiation”. *Nanochem. Res.* Vol, 2, pp.166–171, 2017. [doi: 10.22036/ncr.2017.02.006](https://doi.org/10.22036/ncr.2017.02.006).
- [13] MR Akbarizadeh, M Naderifar, F Mousazadeh, et al., “Cytotoxic activity and Magnetic Behavior of green synthesized iron oxide nanoparticles on brain glioblastoma cells”. *Nanomed Res J.*, vol. 7, pp.99–106, 2022. [doi: 10.22034/nmrj.2022.01.010](https://doi.org/10.22034/nmrj.2022.01.010).
- [14] Miri A, Najafzadeh H, Darroudi M, et al. Iron oxide nanoparticles: biosynthesis, magnetic behavior, cytotoxic effect”. *Chemistry Open* vol.10, pp.327–333, 2021 [doi: 10.1080/16583655.2024.2357820](https://doi.org/10.1080/16583655.2024.2357820).
- [15] N Shahabadi, S Zendehcheshm, D Jamshidi, F Khademi, L Soltani, “Green synthesis of  $\gamma$ -Fe<sub>2</sub>O<sub>3</sub>@SiO<sub>2</sub> magnetic nanoparticles functionalized with penciclovir drug: antiproliferative effect, and nucleic acids (DNA and RNA) interaction”, *Journal of Taibah University for Science*, vol.18, pp. 2357820, 2024 [doi: 10.1080/16583655.2024.2357820](https://doi.org/10.1080/16583655.2024.2357820)

- [16] J. A. A. Abdullah, L. S. Eddine, B. Abderrhmane, et al. "Green synthesis and characterization of iron oxide nanoparticles by pheonix dactylifera leaf extract and evaluation of their antioxidant activity", *Sustain. Chem Pharm.* vol.17, pp. 100280. 2020 doi: [10.1016/j.scp.2020.100280](https://doi.org/10.1016/j.scp.2020.100280).
- [17] R. Rahmani, S. Beaufort, A.S. Villarreal Soto, P. Taillandier, J. Bouajila, M. Debouba, "Kombucha fermentation of African mustard (*Brassica tournefortii*) leaves: Chemical composition and bioactivity", *Food Biosciences*, vol. 30, 2019. doi: [10.1016/j.fbio.2019.100414](https://doi.org/10.1016/j.fbio.2019.100414)
- [18] R. Rahmani, J. Bouajila, M. Jouaidi, M. Debouba, "African mustard (*Brassica tournefortii*) as source of nutrients and nutraceuticals properties". *J. Food Science*, vol.85, no. 6, pp.1856-1871, 2020. doi: [10.1111/1750-3841.15157](https://doi.org/10.1111/1750-3841.15157)
- [19] W.M. Barag, F. A. Shtewi, A.A.U. Tarroush, W.M. Al-Adiwish, M.K. Altounsi, "Green Synthesis of Silver Nanowires Using *Brassica Tournefortii* Leaves Extract and Evaluation of Their Antibacterial and antioxidant Activities", *J.Appl. Organomet. Chem.* vol.5, no.1, pp.13-27, 2025 doi: [10.48309/JAOC.2025.485302.1244](https://doi.org/10.48309/JAOC.2025.485302.1244)
- [20] W.M. Barag, F. A. Shtewi, W.M. Al-Adiwish, A.A.U. Tarroush, "First Report of green Synthesis of Copper Oxide Nanoparticles from *Brassica Tournefortii* Leaves Extract and Their Antibacterial Activity", *Libyan J Med Res.* vol.16, no.2B pp.60-73, 2023 doi: [10.54361/ljmr.16B206,2023](https://doi.org/10.54361/ljmr.16B206,2023)
- [21] I. Khan, K. Saeed, I. Zekker, B. Zhang, A.H. Hendi, A. Ahmad, S. Ahmad, N. Zada, H. Ahmad, L.A. Shah, et al., "Review on Methylene Blue: Its Properties, Uses, Toxicity and Photodegradation". *Water* vol.14, pp.242, 2022 doi:[10.3390/w14020242](https://doi.org/10.3390/w14020242)
- [22] V.H. Rathi, A.R. Jeice, "Green fabrication of nanoparticles using various plant extracts and their multifaceted applications in photocatalytic cationic dye degradation and antimicrobial activities", *Biomass Conversion and Biorefinery.* 2023 doi:[10.1007/s13399-023-04350-2](https://doi.org/10.1007/s13399-023-04350-2)
- [23] N.F. Mott, E.A. Davies, "Electronic Processes in Non-Crystalline Materials, second Edition. Clare don Press, Oxford 1979
- [24] H. Priyadarshi, K. Singh, A. Shrivastava, "Experimental study of maghemite nanoparticles towards sustainable energy storage device application", *materials science in semiconductor processing*, vol.147, pp.106698, 2022 doi:[10.1016/j.mssp.2022.106698](https://doi.org/10.1016/j.mssp.2022.106698)
- [25] Joint Committee on Powder Diffraction Standards (JCPDS), "Cards: FeO [6–711], alpha-Fe<sub>2</sub>O<sub>3</sub> [16–653], Fe<sub>3</sub>O<sub>4</sub> [19–629], g-Fe<sub>2</sub>O<sub>3</sub>[39–1346]".
- [26] D. Cao, H. Li, L. Pan, J. Li, X. Wang, P. Jing, X. Cheng, W. Wang, J. Wang, Q. Liu. "High saturation magnetization of  $\gamma$ -Fe<sub>2</sub>O<sub>3</sub> nano-particles by a facile one-step synthesis approach". *Scientific Reports*, vol. 6, pp. 32360, 2016 doi: [10.1038/srep32360](https://doi.org/10.1038/srep32360)
- [27] A. Zubrik, D. Jáger, E. Mačingová, M. Matik, S. Hredzák, "Spontaneous degradation of methylene blue adsorbed on magnetic biochars". *Scientific Reports* vol.13, pp.14773, 2023 doi:[10.1038/s41598-023-39976-9](https://doi.org/10.1038/s41598-023-39976-9)
- [28] C. Liang, H. Liu, J. Zhou, X. Peng, H. Zhang, "One-Step Synthesis of Spherical  $\gamma$ -Fe<sub>2</sub>O<sub>3</sub> Nanopowders and the Evaluation of Their Photocatalytic Activity for Orange I Degradation". *Journal of Chemistry*, vol. 8, 2015 doi:[10.1155/2015/791829](https://doi.org/10.1155/2015/791829)
- [29] F. Riyanti, H. Hasanudin, A. Rachmat, W. Purwaningrum, P. L. Hariani, "Photocatalytic degradation of methylene blue and Congo red dyes from aqueous solutions by bentonite-Fe<sub>3</sub>O<sub>4</sub> magnetic". *Communications in Science and Technology* Vol. 8, no.1, () pp.1–9, 2023 doi:[10.21924/cst.8.1.2023.1007](https://doi.org/10.21924/cst.8.1.2023.1007)

- [30] S. Boddu, B. P. Marri, R. M. Katika, I. Mikkili, J. B. Dulla, V. N. Allugunulla, S. Malladi, A. A. Khan. “Green Synthesis of Copper Oxide Nanoparticles (CuONPs) using *Ricinus Communis*: Efficient Photocatalytic Dye Degradation and Antibacterial Applications”. *Water Air Soil Pollut.*, 209-236 2025 [doi:10.1007/s11270-025-07841-2](https://doi.org/10.1007/s11270-025-07841-2)

**Disclaimer/Publisher’s Note:** The statements, opinions, and data contained in all publications are solely those of the individual author(s) and contributor(s) and not of **SJPHRT** and/or the editor(s). **SJPHRT** and/or the editor(s) disclaim responsibility for any injury to people or property resulting from any ideas, methods, instructions, or products referred to in the content.